Laurent+Pietarinen Method in Baryon Spectroscopy

M. Hadzimehmedovic, H. Osmanovic, R. Omerovic, J. Stahov, A. Svarc, L. Tiator, R. L. Workman

The International Workshop on Partial Wave Analyses and Advanced Tools for Hadron Spectroscopy (PWA9/Athos4) Bad Honnef, 13 - 17 March 2017

PHYSICAL REVIEW C **88**, 035206 (2013)

Introducing the Pietarinen expansion method into the single-channel pole extraction problem

Alfred Švarc*
Rudjer Bošković Institute, Bijenička cesta 54, P.O. Box 180, 10002 Zagreb, Croatia

Mirza Hadžimehmedović, Hedim Osmanović, and Jugoslav Stahov
University of Tuzla, Faculty of Science, Univerzitetska 4, 75000 Tuzla, Bosnia and Herzegovina

Lothar Tiator
Institut für Kernphyik, Universität Mainz, D-55099 Mainz, Germany

Ron L. Workman
Data Analysis Center at the Institute for Nuclear Studies, Department of Physics, The George Washington University, Washington, D.C. 20052, USA

(Received 19 July 2013; published 20 September 2013)

L+P Method
Laurent expansion

According to Mittag -Leffleur theorem

However, the functions we meet and analyze in reality may and do contain more than one pole for $\omega \neq \omega_0$. So if we iterate this procedure using Mittag-Leffler theorem [4] which says that a meromorphic function can be expressed in terms of its poles and associated residues combined with additional entire function, we can without loss of generality write down the generalized Laurent expansion for the function with k poles:

Our basic assumption is that our amplitudes have only simple first order poles. In that case Laurent expansion may be writen in the following form, where all terms with n<-1 are absent

$$T(\omega) = \frac{(a_R + i\, a_I)_{-1}}{\omega_0 - \omega} + \sum_{n=0}^{\infty} a_n (\omega_0 - \omega)^n$$

In another words it might be writen as

$$T(\omega) = \sum_{i=1}^{k} \frac{a_{-1}^{(i)}}{\omega_i - \omega} + B^L(\omega)$$

L+P Method

In above representation, amplitude, as analytic function, consists of Poles and Background as its regular part.
Analytic structure of background term $B^L(\omega)$ might be "rich" (real or complex branch-points and corresponding cuts)
As an example: Let us show analytic structure of P_{11} partial wave in πN scattering. (z stands for complex energy)

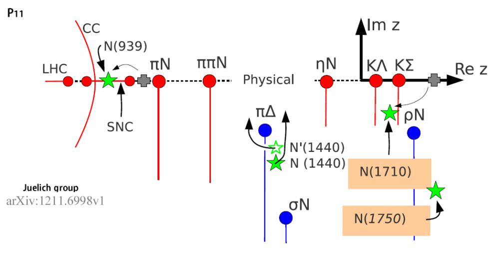

L+P Method

Pietarinen expansion

The basic idea behind Pietarinen expansion method is to represent analytic function in terms of the simplest functions having the same analytic structure.

If $F(\omega)$ is a general, unknown analytic function having a cut starting at $\omega = x_P$, then it can be represented in a power series of Pietarinen functions in the following way:

$$F(\omega) = \sum_{n=0}^{N} c_n \, Z(\omega)^n, \qquad \omega \in \mathbb{C}$$

$$Z(\omega) = \frac{\alpha - \sqrt{x_P - \omega}}{\alpha + \sqrt{x_P - \omega}}, \quad c_n, x_P, \alpha \in \mathbb{R}, \qquad (3)$$

with the α and c_n being tuning parameter and coefficients of Pietarinen function $Z(\omega)$ respectively.

$Z(\omega)$ mapps complex ω-plane into and on unit circle in complex Z plane

L+P Method

Pietarinen expansion

Pietarinen expansion makes it possible to construct an analytic function NOT in the full complex energy plane, but LOCALLY, close to the real axis in the area of dominant nucleon resonances. It has well defined area of convergence.
Example: P_{11} Again,

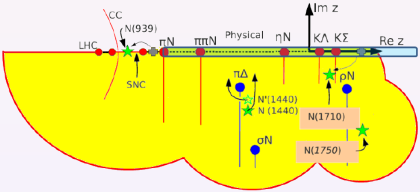

As you may see from above figure, there is a lot of cuts and it would be technically difficult to represent each of them with corresponding Pietarinen series. For this reason we use only three Pietarinen series:

- One to represent subthreshold, unphysical contributions
- Two in physical region to represent all inelastic channel openings

L+P Method

Pietarinen expansion

$$
\begin{aligned}
B^L(\omega) &= \sum_{n=0}^{M} c_n\, Z(\omega)^n + \sum_{n=0}^{N} d_n\, W(\omega)^n + \cdots \\
Z(\omega) &= \frac{\alpha - \sqrt{x_P - \omega}}{\alpha + \sqrt{x_P - \omega}}; \quad W(\omega) = \frac{\beta - \sqrt{x_Q - \omega}}{\beta + \sqrt{x_Q - \omega}} + \cdots \\
& a_{-1}^{(i)}, \omega_i, \omega \in \mathbb{C} \\
& c_n, x_P, d_n, x_Q, \alpha, \beta ... \in \mathbb{R} \\
& \text{and } \; k, M, N ... \in \mathbb{N}. \qquad (4)
\end{aligned}
$$

L+P Method

What can we do with this method?

We may analyze various kinds of inputs:

- Theoretical curves coming from ANY model
- Information coming directly from experiment (partial wave data)

To fit "theoretical input"

we have to “guess” both: pole position and exact analytic structure of the background described by a model

To fit "experimental input"

we have to “guess” only: pole position and the simplest analytic structure of the background. There is no “experimental” information about the background.

PHYSICAL REVIEW C **89**, 045205 (2014)

Poles of Karlsruhe-Helsinki KH80 and KA84 solutions extracted by using the Laurent-Pietarinen method

Alfred Švarc*
Rudjer Bošković Institute, Bijenička cesta 54, P.O. Box 180, 10002, Zagreb, Croatia

Mirza Hadžimehmedović, Rifat Omerović, Hedim Osmanović, and Jugoslav Stahov
University of Tuzla, Faculty of Science, Univerzitetska 4, 75000, Tuzla, Bosnia and Herzegovina
(Received 13 January 2014; revised manuscript received 24 February 2014; published 14 April 2014)

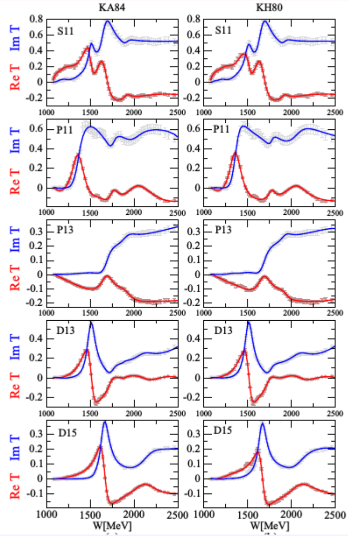

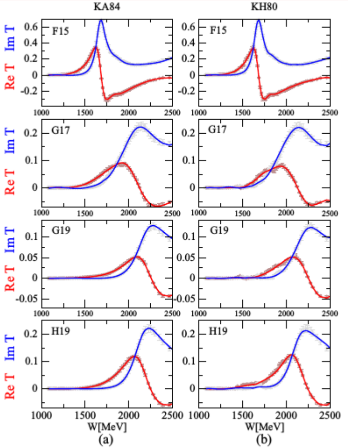

FIG. 2. (Color online) L + P fit for I = 1/2 solutions. (a) Fit to KA84, (b) fit to KH80.

PW	Source	Resonance	Re W_p	$-2\text{Im}\, W_p$	|Residue|	θ
S_{11}	RPP		**1490–1530**	**90–250**	**50 ± 20**	**(−15 ± 15)°**
	RPP H93		**1487**	–	–	–
	KH80 L + P	N(1535) 1/2⁻	1509 ± 4 ± 2	118 ± 9 ± 2	22 ± 2 ± 0.4	(−5 ± 5 ± 3)°
	KA84 L + P		1505 ± 3 ± 1	103 ± 7 ± 3	20 ± 2 ± 1	(−14 ± 3 ± 1)°
	RPP		**1640–1670**	**100–175**	**20–50**	**(−50–80)°**
	RPP H93		**1670**	**163**	**39**	**−37°**
	KH80 L + P	N(1650) 1/2⁻	1660 ± 3.5 ± 1	167 ± 8 ± 2	47 ± 3 ± 1	(−47 ± 3 ± 1)°
	KA84 L + P		1663 ± 3 ± 0	165 ± 7 ± 1	45 ± 2 ± 1	(−44 ± 3 ± 1)°
	RPP		**1900–2150**	**90–479**	**1–60**	**(0–164)°**
	RPP H93		–	–	–	–
	KH80 L + P	N(1895) 1/2⁻	1917 ± 19 ± 1	101 ± 36 ± 1	3.1 ± 1.4 ± 0	(−107 ± 23 ± 2)°
	KA84 L + P		1920 ± 19 ± 2	93 ± 15 ± 3	2.7 ± 1 ± 0.2	(−105 ± 23 ± 3)°
P_{11}	RPP		**1350–1380**	**160–220**	**40–52**	**(−75–100)°**
	RPP H93		**1385**	**164**	**40**	–
	KH80 L + P	N(1440) 1/2⁺	1363 ± 2 ± 2	180 ± 4 ± 5	50 ± 1 ± 2	(−88 ± 1 ± 2)°
	KA84 L + P		1365 ± 2 ± 4	187 ± 4 ± 10	48 ± 1 ± 3	(−88 ± 1 ± 4)°
	RPP		**1670–1770**	**80–380**	**6–15**	**(90–200)°**
	RPP H93		**1690**	**200**	**15**	–
	KH80 L + P	N(1710)* 1/2⁺	1770 ± 5 ± 2	98 ± 8 ± 5	5 ± 1 ± 1	(−104 ± 7 ± 3)°
	KA84 L + P		1763 ± 4 ± 9	105 ± 5 ± 10	6 ± 1 ± 1	(−117 ± 4 ± 15)°
	RPP		**2120 ± 40**	**180 – 420**	**14 ± 7**	**(35 ± 25)°**
	RPP H93		–	–	–	–
	KH80 L + P	N(2100)* 1/2⁺	2052 ± 6 ± 3	337 ± 10 ± 4	30 ± 1 ± 1	(−92 ± 3 ± 2)°
	KA84 L + P		2023 ± 5 ± 25	346 ± 9 ± 13	32 ± 1 ± 3	(−118 ± 3 ± 21)°
P_{13}	RPP		**1660–1690**	**150–400**	**15 ± 8**	**(−130 ± 30)°**
	RPP H93		**1686**	**187**	**15**	–
	KH80 L + P	N(1720) 3/2⁺	1677 ± 4 ± 1	184 ± 8 ± 1	13 ± 1 ± 0	(−115 ± 3 ± 2)°
	KA84 L + P		1685 ± 4 ± 1	178 ± 8 ± 1	13 ± 1 ± 1	(−104 ± 4 ± 1)°
	RPP		**1870–1930**	**140–300**	**3 ± 2**	**(10 ± 35)°**
	RPP H93		–	–	–	–
	KH80 L + P	N(1900)* 3/2⁺	1928 ± 18 ± 2	152 ± 40 ± 9	4 ± 1 ± 1	(−29 ± 15 ± 2)°
	KA84 L + P		1920 ± 17 ± 1	215 ± 37 ± 2	7 ± 1 ± 1	(−38 ± 11 ± 1)°

N(1440) POLE POSITION

REAL PART

VALUE (MeV)	*DOCUMENT ID*		*TECN*	*COMMENT*
1369 ± 3	SOKHOYAN	15A	DPWA	Multichannel
1363 ± 2 ± 2	[1] SVARC	14	L+P	$\pi N \to \pi N$
1359	ARNDT	06	DPWA	$\pi N \to \pi N, \eta N$
1385	HOEHLER	93	SPED	$\pi N \to \pi N$
1375 ± 30	CUTKOSKY	80	IPWA	$\pi N \to \pi N$

• • • We do not use the following data for averages, fits, limits, etc. • • •

PHYSICAL REVIEW C **89**, 065208 (2014)

Pole positions and residues from pion photoproduction using the Laurent-Pietarinen expansion method

Alfred Švarc*
Rudjer Bošković Institute, Bijenička cesta 54, P.O. Box 180, 10002 Zagreb, Croatia

Mirza Hadžimehmedović, Hedim Osmanović, and Jugoslav Stahov
University of Tuzla, Faculty of Science, Univerzitetska 4, 75000 Tuzla, Bosnia and Herzegovina

Lothar Tiator
Institut für Kernphysik, Universität Mainz, D-55099 Mainz, Germany

Ron L. Workman
Data Analysis Center at the Institute for Nuclear Studies, Department of Physics, The George Washington University, Washington, D.C. 20052, USA
(Received 14 April 2014; published 20 June 2014)

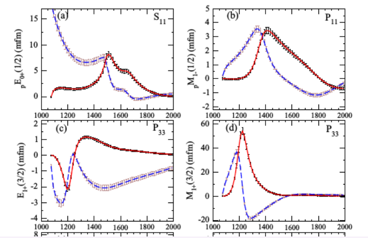

FIG. 1. (Color online) L + P fit to GWU-SAID CM12 ED solutions.

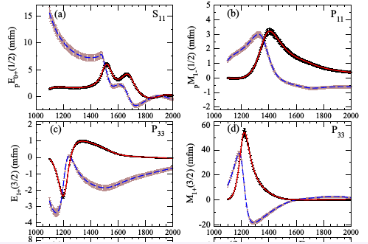

FIG. 2. (Color online) L + P fit to MAID MAID2007 ED solutions.

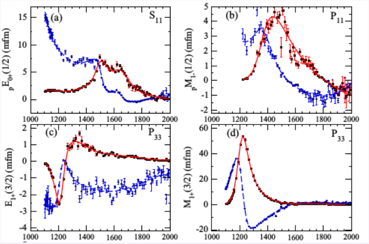

FIG. 4. (Color online) L + P fit to GWU-SAID CM12 SE solutions.

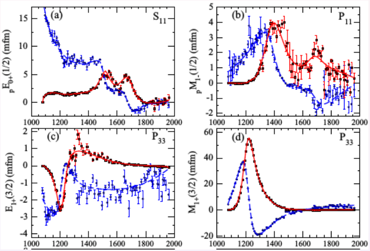

FIG. 3. (Color online) L + P fit to MAID MAID2007 SE solutions.

TABLE I. Pole positions in MeV and residues of four dominant isospin 1/2 multipoles as moduli in mfm GeV and phases in degrees for real branch points. The results from L + P expansion are given for GWU-SAID and MAID energy-dependent (ED) and single-energy (SE) solutions. Resonances marked with a star indicate resonances which can be alternatively explained by the ρN complex branch point. Empty lines indicate that a resonance pole could not be found with a significant statistical weight.

Multipole	Source	Resonance	$\mathrm{Re}W_p$	$-2\mathrm{Im}W_p$	|Residue|	θ
$S_{11}(_pE_{0+})$	SAID ED	$N(1535)\ 1/2^-$	$1501 \pm 4 \pm 2$	$95 \pm 9 \pm 2$	$0.245 \pm 0.030 \pm 0.008$	$-(25 \pm 7 \pm 3)^\circ$
	MAID ED		$1516 \pm 1 \pm 2$	$94 \pm 3 \pm 2$	$0.234 \pm 0.009 \pm 0.004$	$-(2 \pm 3 \pm 7)^\circ$
	MAID SE		$1511 \pm 1 \pm 6$	$93 \pm 2 \pm 7$	$0.210 \pm 0.002 \pm 0.021$	$-(5 \pm 1 \pm 7)^\circ$
	SAID SE		$1501 \pm 1 \pm 2$	$112 \pm 2 \pm 7$	$0.312 \pm 0.003 \pm 0.022$	$-(18 \pm 1 \pm 3)^\circ$
	SAID ED	$N(1650)\ 1/2^-$	$1655 \pm 8 \pm 3$	$127 \pm 10 \pm 7$	$0.119 \pm 0.019 \pm 0.013$	$-(18 \pm 14 \pm 9)^\circ$
	MAID ED		$1678 \pm 2 \pm 2$	$135 \pm 3 \pm 2$	$0.289 \pm 0.010 \pm 0.009$	$+(12 \pm 3 \pm 4)^\circ$
	MAID SE		$1681 \pm 1 \pm 3$	$113 \pm 1 \pm 6$	$0.231 \pm 0.001 \pm 0.024$	$-(21 \pm 1 \pm 6)^\circ$
	SAID SE		$1650 \pm 1 \pm 1$	$117 \pm 2 \pm 14$	$0.153 \pm 0.002 \pm 0.026$	$-(8 \pm 5 \pm 5)^\circ$
	SAID ED	$N(1895)\ 1/2^-$	–	–	–	–
	MAID ED		$1913 \pm 4 \pm 8$	$258 \pm 10 \pm 37$	$0.327 \pm 0.015 \pm 0.2$	$-(68 \pm 4 \pm 10)^\circ$
	MAID SE		–	–	–	–
	SAID SE		–	–	–	–
$P_{11}(_pM_{1-})$	SAID ED	$N(1440)\ 1/2^+$	$1360 \pm 4 \pm 1$	$183 \pm 10 \pm 9$	$0.290 \pm 0.015 \pm 0.039$	$-(61 \pm 4 \pm 1)^\circ$
	MAID ED		$1367 \pm 1 \pm 1$	$190 \pm 3 \pm 2$	$0.306 \pm 0.011 \pm 0.004$	$-(44 \pm 4 \pm 1)^\circ$
	MAID SE		$1379 \pm 2 \pm 4$	$183 \pm 3 \pm 5$	$0.394 \pm 0.003 \pm 0.005$	$-(36 \pm 1 \pm 5)^\circ$
	SAID SE		$1367 \pm 2 \pm 8$	$235 \pm 3 \pm 8$	$0.547 \pm 0.006 \pm 0.052$	$-(75 \pm 1 \pm 6)^\circ$
	SAID ED	$N(1710)^*\ 1/2^+$	$1789 \pm 9 \pm 4$	$550 \pm 25 \pm 3$	$0.609 \pm 0.031 \pm 0.014$	$+(98 \pm 3 \pm 4)^\circ$
	MAID ED		$1694 \pm 22 \pm 12$	$269 \pm 44 \pm 35$	$0.029 \pm 0.005 \pm 0.008$	$+(65 \pm 5 \pm 9)^\circ$
	MAID SE		$1678 \pm 5 \pm 3$	$99 \pm 14 \pm 23$	$0.062 \pm 0.006 \pm 0.012$	$-(16 \pm 4 \pm 2)^\circ$
	SAID SE		–	–	–	–
$D_{13}(_pE_{2-})$	SAID ED	$N(1520)\ 3/2^-$	$1514 \pm 1 \pm 0$	$109 \pm 4 \pm 1$	$0.373 \pm 0.017 \pm 0.010$	$+(16 \pm 2 \pm 1)^\circ$
	MAID ED		$1509 \pm 1 \pm 0$	$106 \pm 1 \pm 1$	$0.375 \pm 0.003 \pm 0.001$	$+(11 \pm 1 \pm 1)^\circ$
	MAID SE		$1514 \pm 1 \pm 4$	$120 \pm 1 \pm 6$	$0.385 \pm 0.005 \pm 0.024$	$+(12 \pm 1 \pm 2)^\circ$
	SAID SE		$1514 \pm 1 \pm 1$	$111 \pm 1 \pm 0.5$	$0.382 \pm 0.004 \pm 0.003$	$+(14 \pm 1 \pm 3)^\circ$
	SAID ED	$N(1700)^*\ 3/2^-$	$1638 \pm 13 \pm 13$	$362 \pm 24 \pm 17$	$0.382 \pm 0.032 \pm 0.059$	$+(4 \pm 5 \pm 11)^\circ$
	MAID ED		–	–	–	–
	MAID SE		–	–	–	–
	SAID SE		$1654 \pm 5 \pm 15$	$257 \pm 10 \pm 47$	$0.187 \pm 0.007 \pm 0.080$	$-(1 \pm 3 \pm 7)^\circ$
$F_{15}(_pE_{3-})$	SAID ED	$N(1680)\ 5/2^+$	$1674 \pm 2 \pm 0.5$	$113 \pm 4 \pm 0$	$0.157 \pm 0.008 \pm 0$	$-(5 \pm 3 \pm 0)^\circ$
	MAID ED		$1663 \pm 1 \pm 0$	$118 \pm 2 \pm 1$	$0.150 \pm 0.003 \pm 0.001$	$-(3 \pm 1 \pm 1)^\circ$
	MAID SE		$1669 \pm 1 \pm 1$	$113 \pm 1 \pm 1$	$0.145 \pm 0.005 \pm 0.002$	$+(2 \pm 1 \pm 1)^\circ$
	SAID SE		$1677 \pm 1 \pm 1$	$115 \pm 1 \pm 3$	$0.174 \pm 0.002 \pm 0.008$	$+(1 \pm 1 \pm 2)^\circ$
	SAID ED	$N(2000)^*\ 5/2^+$	–	–	–	–
	MAID ED		$1801 \pm 14 \pm 4$	$141 \pm 28 \pm 13$	$0.007 \pm 0.002 \pm 0.003$	$+(32 \pm 14 \pm 9)^\circ$
	MAID SE		–	–	–	–

PHYSICAL REVIEW C **91**, 015207 (2015)

Pole structure from energy-dependent and single-energy fits to GWU-SAID πN elastic scattering data

Alfred Švarc*
Rudjer Bošković Institute, Bijenička cesta 54, Post Office Box 180, 10002 Zagreb, Croatia

Mirza Hadžimehmedović, Hedim Osmanović, and Jugoslav Stahov
University of Tuzla, Faculty of Science, Univerzitetska 4, 75000 Tuzla, Bosnia and Herzegovina

Ron L. Workman
Data Analysis Center at the Institute for Nuclear Studies, Department of Physics, George Washington University, Washington, D.C. 20052, USA
(Received 28 May 2014; revised manuscript received 23 December 2014; published 29 January 2015)

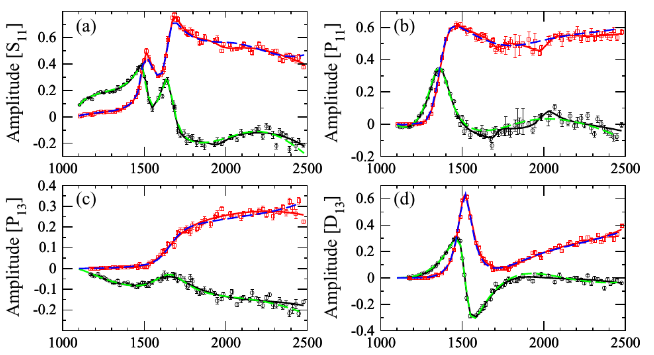
(a)
Amplitude [S_{11}]
0.6
0.4
0.2
0
-0.2
1000
1500
2000
2500
(b)
Amplitude [P_{11}]
0.6
0.4
0.2
0
-0.2
1000
1500
2000
2500
(c)
Amplitude [P_{13}]
0.4
0.3
0.2
0.1
0
-0.1
-0.2
1000
1500
2000
2500
(d)
Amplitude [D_{13}]
0.6
0.4
0.2
0
-0.2
-0.4
1000
1500
2000
2500

PW	Resonance	Source	Re W_p	$-2\text{Im } W_p$	|residue|	θ
S_{11}	$N(1535)\ 1/2^-$	**RPP**	**1490–1510**	**90–170**	**50 ± 20**	**(−15 ± 15)°**
		WI08	**1499**	**98**	**17**	**−24°**
		WI08 ED L+P	1497 ± 8 ± 1	85 ± 14 ± 7	13 ± 3 ± 1	−(41 ± 12 ± 4)°
		WI08 SE L+P	1507 ± 1 ± 0	88 ± 3 ± 1	17 ± 0.6 ± 0.2	−(22 ± 2 ± 2)°
	$N(1650)\ 1/2^-$	**RPP**	**1640–1655**	**100–135**	**40–46**	**(−75 ± 25)°**
		WI08	**1647**	**83**	**15**	**−74°**
		WI08 ED L+P	1645 ± 1 ± 4	94 ± 9 ± 1	20 ± 3 ± 1	−(77 ± 7 ± 2)°
		WI08 SE L+P	1654 ± 2 ± 1	112 ± 4 ± 4	27 ± 1 ± 2	−(57 ± 2 ± 2)°
	$N(1895)^*\ 1/2^-$	**RPP**	**1900–2150**	**90–479**	**1–60**	**(0–164)°**
		WI08				
		WI08 ED L+P				
		WI08 SE L+P	1950 ± 16 ± 6	170 ± 37 ± 23	6 ± 1 ± 1	(97 ± 10 ± 5)°
P_{11}	$N(1440)\ 1/2^+$	**RPP**	**1350–1365**	**160–190**	**40–52**	**(−100 ± 35)°**
		WI08	**1358**	**160**	**37**	**−98°**
		WI08 ED L+P	1358 ± 2 ± 1	180 ± 6 ± 1	45 ± 1 ± 1	−(91 ± 1 ± 1)°
		WI08 SE L+P	1364 ± 0.7 ± 0.3	182 ± 1 ± 0.5	45 ± 0.4 ± 0.3	−(86 ± 0.5 ± 0.3)°
	$N(1710)^*\ 1/2^+$	**RPP**	**1670–1720**	**80–230**	**6–15**	**(90–200)°**
		WI08				
		WI08 ED L+P				
		WI08 SE L+P	1711 ± 10 ± 0.6	84 ± 20 ± 2	2 ± 0.7 ± 0.1	(171 ± 14 ± 0.4)°
	$N(2100)^*\ 1/2^+$	**RPP**	**2120 ± 40**	**180–420**	**14 ± 7**	**(35 ± 25)°**
		WI08				
		WI08 ED L+P				
		WI08 SE L+P	2004 ± 10 ± 1.3	140 ± 20 ± 1.2	7 ± 0 ± 9	−(126 ± 22 ± 1)°
P_{13}	$N(1720)\ 3/2^+$	**RPP**	**1660–1690**	**150–400**	**15 ± 8**	**(−130 ± 30)°**
		WI08	**1661**	**304**	**21**	**−89°**
		WI08 ED L+P	1659 ± 10 ± 1	303 ± 18 ± 1	20 ± 2 ± 1	−(91 ± 6 ± 1)°
		WI08 SE L+P	1668 ± 15 ± 9	303 ± 18 ± 40	16 ± 1 ± 6	−(82 ± 4 ± 8)°

Physics Letters B 755 (2016) 452–455

Generalization of the model-independent Laurent–Pietarinen single-channel pole-extraction formalism to multiple channels

Alfred Švarc [a,*], Mirza Hadžimehmedović [b], Hedim Osmanović [b], Jugoslav Stahov [b], Lothar Tiator [c], Ron L. Workman [d]

[a] Rudjer Bošković Institute, Bijenička cesta 54, P.O. Box 180, 10002 Zagreb, Croatia
[b] University of Tuzla, Faculty of Science, Univerzitetska 4, 75000 Tuzla, Bosnia and Herzegovina
[c] Institut für Kernphyik, Universität Mainz, D-55099 Mainz, Germany
[d] Data Analysis Center at the Institute for Nuclear Studies, Department of Physics, The George Washington University, Washington, DC 20052, United States

$$T^a(W) = \sum_{i=1}^{k} \frac{x_i^a + \imath\, y_i^a}{W_i - W} + \sum_{l=0}^{L^a} c_l^a X^a(W)^l + \sum_{m=0}^{M^a} d_m^a Y^a(W)^m + \sum_{n=0}^{N^a} e_n^a Z^a(W)^n$$

$$X^a(W) = \frac{\alpha^a - \sqrt{x_P^a - W}}{\alpha^a + \sqrt{x_P^a - W}}; \quad Y^a(W) = \frac{\beta^a - \sqrt{x_Q^a - W}}{\beta^a + \sqrt{x_Q^a - W}};$$

$$Z^a(W) = \frac{\gamma^a - \sqrt{x_R^a - W}}{\gamma^a + \sqrt{x_R^a - W}}$$

$$D_{dp} = \sum_a^{all} D_{dp}^a$$

$$D_{dp}^a = \frac{1}{2\,N_{data}} \sum_{i=1}^{N_{data}} \left\{ \left[\frac{\mathrm{Re}\,T^a(W_i) - \mathrm{Re}\,T_{exp}^a(W_i)}{Err_{i,a}^{\mathrm{Re}}} \right]^2 + \left[\frac{\mathrm{Im}\,T^a(W_i) - \mathrm{Im}\,T_{exp}^a(W_i)}{Err_{i,a}^{\mathrm{Im}}} \right]^2 \right\} + \mathcal{P}^a + \mathcal{U}^a$$

$\mathcal{P}^a$ and $\mathcal{U}^a$ … Pietarinen and unitarity penalty functions

$Err_{i,a}^{\mathrm{Re,\,Im}}$ … minimization error of real and imaginary part respectively,

a … correlated quantity index ($\pi N \to \pi N$, $\pi N \to \eta N$, $E_{l\pm}$, $M_{l\pm}$ …)

L^a, M^a, N^a … $\in \mathbb{N}$ number of Pietarinen coefficients in channel a

W_i, $W \in \mathbb{C}$

x_i^a, y_i^a, c_l^a, d_m^a, e_n^a, α^a, β^a, γ^a … $\in \mathbb{R}$

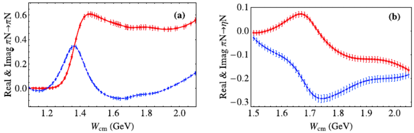

Fig. 1. (Color online.) The SC L+P result for BG2011-2 [17,18] $\pi N \to \pi N$ and $\pi N \to \eta N$ P_{11} PW amplitudes is shown in (a) and (b) respectively. Blue and red full and dashed lines give the real and imaginary parts respectively.

Table 1
Two independent SC L+P analyses of πN elastic and $\pi N \to \eta N$ BG 2011-2 amplitudes. M_i and Γ_i are the resonance position and width; $|a_i^a|$ and θ_i^a give the residue in terms of modulus and phase.

Fitted channel	Resonance name	M_i	Γ_i	$\lvert a_i^a \rvert$	θ_i^a	D_{dp}^a
πN elastic	N(1440)1/2+	1368	193	49	−82	0.004
two poles	N(1880)1/2+	1857	321	15	179	
$\pi N \to \eta N$	N(1710)1/2+	1686	204	19	−27	0.002
two poles	N(1880)1/2+	1861	252	20	−95	

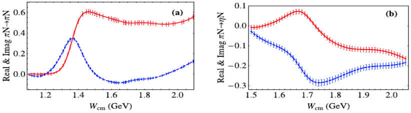

Fig. 2. (Color online.) The MC L+P result for BG2011-2 [17,18] $\pi N \to \pi N$ and $\pi N \to \eta N$ P_{11} PW amplitudes is shown in (a) and (b) respectively. Blue and red full and dashed lines give the real and imaginary parts respectively.

Table 2
Comparison of published theoretical BG2011-2 [17,18] pole parameters with MC L+P results. M_i and Γ_i are the resonance position and width; $|a_i^a|$ and θ_i^a give the residue in terms of modulus and phase.

Resonance name		PDG [1]	BG[17,18]	$BG^{MC\ L+P}$
N(1440)1/2+	M_1	1350–1380	1370(4) [17]	1368(3)
	Γ_1	160–220	190(7)	191(3)
	$\|a\|_1^{\pi N}$	40–52	48(3)	49(2)
	$\Theta_1^{\pi N}$	75–100	−78(4)	−82(3)
	$\frac{2\|a\|_1^{\eta N}}{\Gamma}$	-	-	0.1(0.1)%
	$\Theta_1^{\eta N}$	-	-	22(20)
N(1710)1/2+	M_2	1670–1770	1687(17) [17]	1686(8)
	Γ_2	80–330	200(25)	153(24)
	$\|a\|_2^{\pi N}$	6–15	6(4)	2(1)
	$\Theta_2^{\pi N}$	120–193	120(70)	155(21)
	$\frac{2\|a\|_2^{\eta N}}{\Gamma}$	-	12(4)%	14(3)%
	$\Theta_2^{\eta N}$	-	0(45)	21(7)
N(1880)1/2+	M_3	1860(35)	1860(35)[17]	1875(9)
	Γ_3	250(70)	250(70)	232(15)
	$\|a\|_3^{\pi N}$	6(4)	6(4)	3(1)
	$\Theta_3^{\pi N}$	80(65)	80(65)	107(16)
	$\frac{2\|a\|_3^{\eta N}}{\Gamma}$	-	11(7)%	6(1)%
	$\Theta_3^{\eta N}$	-	−75(55)	−131(26)
N(2100)1/2+	M_4	2120(40)	2100 [18]	2171(24)

PHYSICAL REVIEW C **94**, 065204 (2016)

Baryon transition form factors at the pole

L. Tiator,[1] M. Döring,[2,3] R. L. Workman,[2] M. Hadžimehmedović,[4] H. Osmanović,[4] R. Omerović,[4] J. Stahov,[4] and A. Švarc[5]

[1] *Institut für Kernphysik, Universität Mainz, D-55099 Mainz, Germany*
[2] *The George Washington University, Washington, DC 20052, USA*
[3] *Thomas Jefferson National Accelerator Facility, Newport News, Virginia 23606, USA*
[4] *University of Tuzla, Faculty of Natural Sciences and Mathematics, Univerzitetska 4, 75000 Tuzla, Bosnia and Herzegovina*
[5] *Rudjer Bošković Institute, Bijenička Cesta 54, P.O. Box 180, 10002 Zagreb, Croatia*

(Received 11 June 2016; published 21 December 2016)

$$G_M^{\text{pole}}(Q^2) = b_p(Q^2)\,\text{Res}\, M_{1+}^{(3/2)}(W_p, Q^2),$$
$$G_E^{\text{pole}}(Q^2) = -b_p(Q^2)\,\text{Res}\, E_{1+}^{(3/2)}(W_p, Q^2),$$
$$G_C^{\text{pole}}(Q^2) = -b_p(Q^2)\frac{2W_p}{k_p(Q^2)}\,\text{Res}\, S_{1+}^{(3/2)}(W_p, Q^2),$$

$$R_{EM}^{\text{pole}}(Q^2) = \frac{\text{Res}\, E_{1+}^{3/2}(Q^2)}{\text{Res}\, M_{1+}^{3/2}(Q^2)} = -\frac{G_E^{\text{pole}}(Q^2)}{G_M^{\text{pole}}(Q^2)},$$
$$R_{SM}^{\text{pole}}(Q^2) = \frac{\text{Res}\, S_{1+}^{3/2}(Q^2)}{\text{Res}\, M_{1+}^{3/2}(Q^2)} = -\frac{k_p(Q^2)}{2W_p}\frac{G_C^{\text{pole}}(Q^2)}{G_M^{\text{pole}}(Q^2)}.$$

$$A_h^{\text{pole}} = C\sqrt{\frac{q_p}{\kappa_p}\frac{2\pi(2J+1)W_p}{m_N \text{Res}_{\pi N}}}\ \text{Res}\,\mathcal{A}_\alpha^h,$$
$$S_{1/2}^{\text{pole}} = C\sqrt{\frac{q_p}{\kappa_p}\frac{2\pi(2J+1)W_p}{m_N \text{Res}_{\pi N}}}\ \text{Res}\,\mathcal{S}_\alpha^{1/2},$$

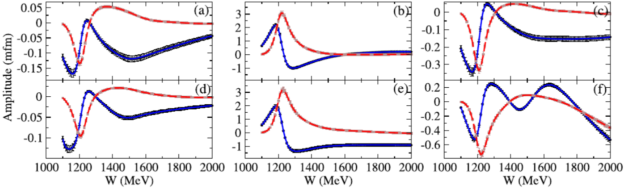

FIG. 1. Figures showing the quality of the fit. From top to bottom we show all three multipoles at three different photon virtualities $Q^2 = 0$, 1, and 5 GeV^2 for MAID2007 and SAID SM08 models. Black circles and brown squares are real and imaginary part of multipoles respectively. Blue solid lines are real parts and red dashed lines are imaginary parts of the L+P fit to the given model. Panels (a)–(c) show $E_{1+}^{3/2}, M_{1+}^{3/2}, S_{1+}^{3/2}$ of the MAID solution and (d)–(f) the same for the SAID solution.

TABLE I. Magnetic, electric and charge transition form factors, E/M, S/M ratios and photon decay amplitudes at $Q^2 = 0$ for the Breit-Wigner and for the pole position compared between MAID and SAID solutions. The BW parameters used for the conversion factor are $M_\Delta = 1232$ MeV and $\Gamma_\pi = \Gamma_r = 115$ MeV, and the pole parameters are $W_p = (1210 - 50i)$ MeV and $\mathrm{Res}_{\pi N} = 50\, e^{-i47^\circ}$. The form factors and ratios are dimensionless and the photon decay amplitudes are given in units of $\mathrm{GeV}^{-1/2}$. For the complex values at the pole position, we give absolute values with the same sign as for the BW values and a phase.

	MAID values			SAID values		
	BW	pole		BW	pole	
G_M	2.97	3.20	-4.7°	3.11	3.38	-3.5°
G_E	0.064	0.202	49°	0.051	0.181	54°
G_C	1.18	2.11	35°	1.30	2.31	34°
R_{EM}	-0.022	-0.063	53°	-0.016	-0.054	58°
R_{SM}	-0.042	-0.067	33°	-0.044	-0.069	30°
$A_{1/2}$	-0.131	-0.131	-20°	-0.139	-0.142	-18°
$A_{3/2}$	-0.247	-0.261	-7.7°	-0.258	-0.273	-6.8°
$S_{1/2}$	0.016	0.027	22°	0.018	0.030	21°

$\gamma p \to K^+\Lambda$

First (nearly) model-independent confirmation of resonances in the fourth resonance region

A.V. Anisovich,[1,2] V. Burkert,[3] M. Hadžimehmedović,[4] D.G. Ireland,[4] E. Klempt,[1,3] V.A. Nikonov,[1,2] R. Omerović,[5] H. Osmanović,[5] A.V. Sarantsev,[1,2] J. Stahov,[5] A. Švarc,[6] and U. Thoma[1]

[1] *Helmholtz–Institut für Strahlen– und Kernphysik, Universität Bonn, 53115 Bonn, Germany*
[2] *National Research Centre "Kurchatov Institute", Petersburg Nuclear Physics Institute, Gatchina, 188300 Russia*
[3] *Thomas Jefferson National Accelerator Facility, Newport News, Virginia 23606, USA*
[4] *University of Glasgow, Glasgow G12 8QQ, United Kingdom*
[5] *University of Tuzla, Faculty of Science, Univerzitetska 4, 75000 Tuzla, Bosnia and Herzegovina*
[6] *Rudjer Boskovic Institute, Bijenicka cesta 54, P.O. Box 180, 10002 Zagreb, Croatia*

$\gamma p \to K^+\Lambda$

Data Base

- $\mathrm{d}\sigma/\mathrm{d}\Omega$ [1,2],
- beam assymetry Σ [3],
- recoil polarization P [3],
- target polarization T [3],
- beam recoil double polarizations Ox [3] and Oz [3].

1. [1] CLAS 2010
2. [2] MAMI
3. [3] CLAS 2015

$\gamma p \to K^+\Lambda$

Model

1. Unconstrained fit for $E0+$, $M1-$, $E1+$, and $M1+$,
2. Partially constrained fit for $E2-$,
3. All higher partial waves from Bonn-Gatchina BG2014-2

$\gamma p \to K^+ \Lambda$

Results of SE Analysis

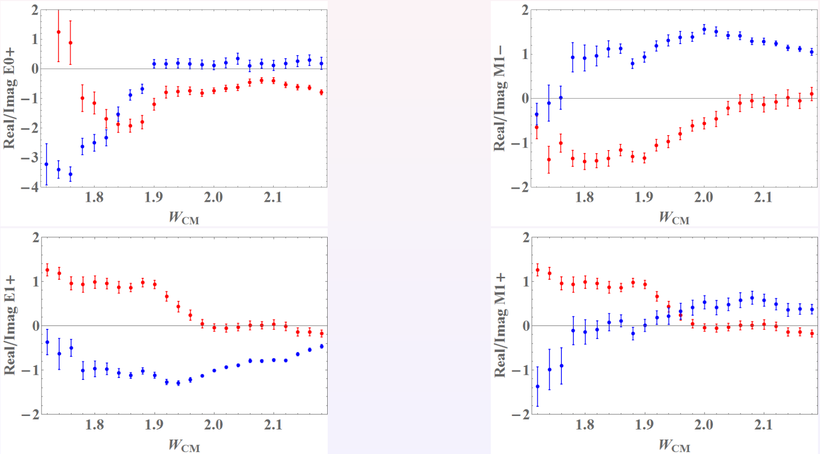

$\gamma p \to K^+\Lambda$

Pole extraction

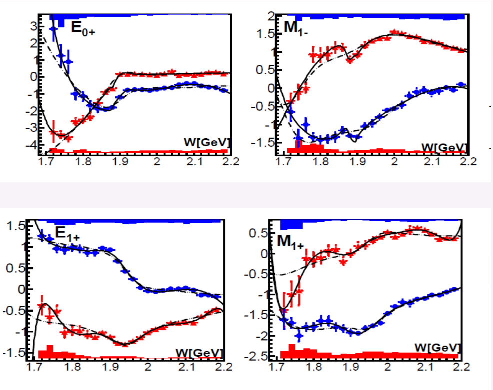

Real (red triangles) and imaginary (blue dots) part of the E_{0+}, M_{1-}, E_{1+} and M_{1+} multipoles for the reaction $\gamma p \to K^+\Lambda$. The systematic errors are given at the top (real part) and bottom (imaginary part) of the subfigures. E_{0+} excites the partial wave $J^P = 1/2^-$; M_{1-}: $J^P = 1/2^+$; E_{1+} and M_{1+}: $J^P = 3/2^+$. The solid curve shows the L+P fit, the dashed curve the energy dependent BnGa fit

$\gamma p \to K^+\Lambda$

Results

Table I. Properties of nucleon resonances from the Particle Data Group (PDG estimates) [14], the BnGa PWA fit, and from $L+P$ fits. Masses and widths are given in MeV, the normalized inelastic pole residues $2 \cdot g^a(\pi N \to K\Lambda)/\Gamma_a$ are numbers.

	$J^P = 1/2^-$			$J^P = 1/2^+$			$J^P = 3/2^+$		
	PDG	BnGa	MC $L+P$	PDG	BnGa	MC $L+P$	PDG	BnGa	L+P
M_1	1640-1670	1658 ± 10	1660 ± 5	1670-1770	1690 ± 15	1697 ± 23	-	-	-
Γ_1	100-170	102 ± 8	59 ± 16	90-380	155 ± 25	84 ± 34	-	-	-
$\lvert Res_1(\pi N \to K\Lambda)\rvert$		0.26 ± 0.10	0.10 ± 0.10	-	0.16 ± 0.05	$0.12^{+0.24}_{-0.12}$	-	-	-
Θ_1	-	$(110 \pm 20)^0$	$(95 \pm 33)^0$	-	$-(160 \pm 25)^0$	$-(119 \pm 83)^0$	-	-	-
M_2	-	1895 ± 15	1906 ± 17	-	1860 ± 40	1875 ± 11	1900-1940	1945 ± 35	1912 ± 30
Γ_2	-	132 ± 30	100 ± 10	-	230 ± 50	33 ± 9	130-300	135^{+70}_{-30}	166 ± 30
$\lvert Res_2(\pi N \to K\Lambda)\rvert$	-	0.09 ± 0.03	0.06 ± 0.02	-	0.05 ± 0.02	0.30 ± 0.10	-	0.03 ± 0.02	–
Θ_2	-	$(8 \pm 30)^0$	$(87 \pm 27)^0$	-	$(27 \pm 30)^0$	$(82 \pm 9)^0$	-	$(90 \pm 40)^0$	–

MC: $1/2^-$ E0+ $\gamma p \to K^+\Lambda$ & corr. $\pi^- p \to \Lambda K^0$ EPJ 2013
MC: $1/2^+$ M1- $\gamma p \to K^+\Lambda$ & corr. od $\pi^- p \to \Lambda K^0$ EPJ 2013

Eur. Phys. J. A (2013) **49**: 121
DOI 10.1140/epja/i2013-13121-9

THE EUROPEAN PHYSICAL JOURNAL A

Regular Article – Experimental Physics

Study of ambiguities in $\pi^- p \to \Lambda K^0$ scattering amplitudes

A.V. Anisovich[1,2], R. Beck[1], E. Klempt[1,a], V.A. Nikonov[1,2], A.V. Sarantsev[1,2], U. Thoma[1], and Y. Wunderlich[1]

[1] Helmholtz-Institut für Strahlen- und Kernphysik, Universität Bonn, Germany
[2] Petersburg Nuclear Physics Institute, Gatchina, Russia

MC L+P

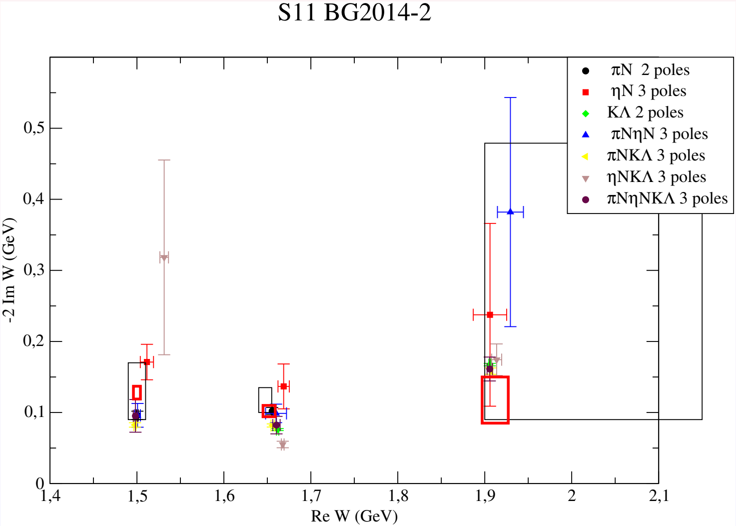
S11 BG2014-2
πN 2 poles
ηN 3 poles
KΛ 2 poles
πNηN 3 poles
πNKΛ 3 poles
ηNKΛ 3 poles
πNηNKΛ 3 poles
-2 Im W (GeV)
Re W (GeV)
0
0,1
0,2
0,3
0,4
0,5
1,4
1,5
1,6
1,7
1,8
1,9
2
2,1

MC L+P

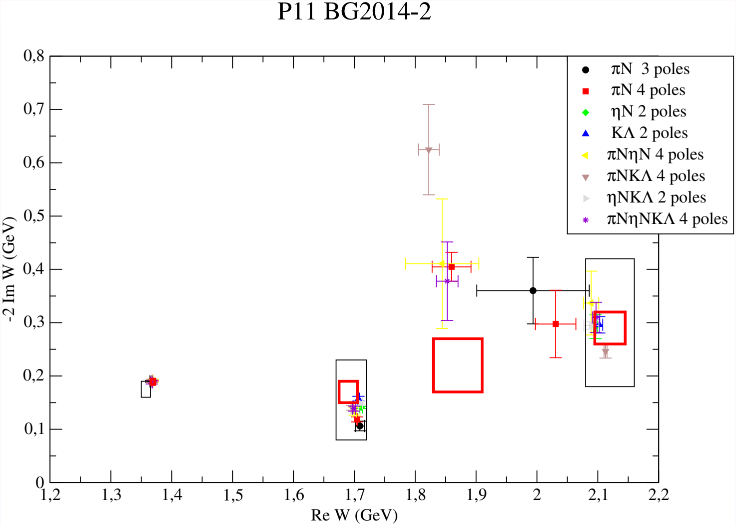
P11 BG2014-2
0,8
0,7
0,6
0,5
0,4
0,3
0,2
0,1
0
-2 Im W (GeV)
1,2
1,3
1,4
1,5
1,6
1,7
1,8
1,9
2
2,1
2,2
Re W (GeV)
πN 3 poles
πN 4 poles
ηN 2 poles
KΛ 2 poles
πNηN 4 poles
πNKΛ 4 poles
ηNKΛ 2 poles
πNηNKΛ 4 poles

MC L+P

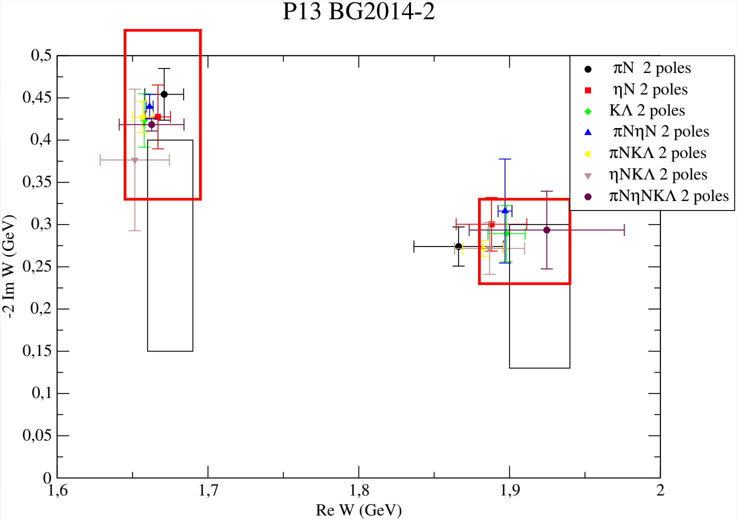
P13 BG2014-2
0,5
0,45
0,4
0,35
0,3
0,25
0,2
0,15
0,1
0,05
0
1,6
1,7
1,8
1,9
2
-2 Im W (GeV)
Re W (GeV)
πN 2 poles
ηN 2 poles
KΛ 2 poles
πNηN 2 poles
πNKΛ 2 poles
ηNKΛ 2 poles
πNηNKΛ 2 poles

MC L+P

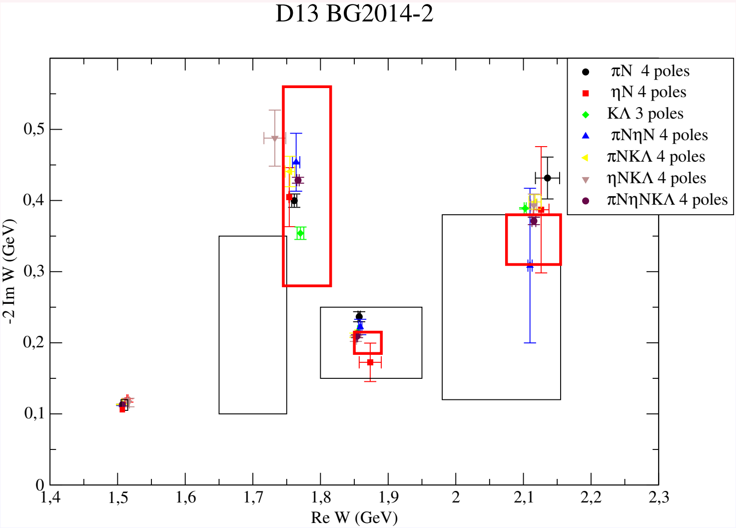
D13 BG2014-2
-2 Im W (GeV)
Re W (GeV)
0
0,1
0,2
0,3
0,4
0,5
1,4
1,5
1,6
1,7
1,8
1,9
2
2,1
2,2
2,3
πN 4 poles
ηN 4 poles
KΛ 3 poles
πNηN 4 poles
πNKΛ 4 poles
ηNKΛ 4 poles
πNηNKΛ 4 poles